DOI: 10.61782/fa.2025.0135

FORUM ACUSTICUM EURONOISE 2025

ANALYTICAL AND EXPERIMENTAL INVESTIGATION OF STATOR ASSEMBLY VIBRATIONS IN ELECTRIC MOTORS

Panagiotis Andreou[1] **Amal Z. Hajjaj**[1] **Mahdi Mohammadpour**[1]
Stephanos Theodossiades[1*]
[1] Loughborough University, School of Mechanical, Electrical and Manufacturing Engineering, Loughborough University, UK

ABSTRACT

This work presents a novel analytical model for the stator of an electric motor, modelled as a thick segmented cylindrical shell, to accurately capture its vibrational behaviour. The methodology employs the First-order Shear Deformation Stress Theory (FSDST) with considerations of mechanical property anisotropies and dimensional variations to represent the system's complex dynamics. An Experimental Modal Analysis (EMA) was performed using an impulse hammer, to identify the stator's modal characteristics. The analytical model demonstrated exceptional accuracy in capturing these features. The experimental results were used to enhance the Rayleigh damping approximation implemented in the model. The enhanced model was applied to predict the forced response of the system under impulse excitation. Comparisons between analytical predictions and experimental measurements revealed excellent agreement, validating the model's reliability in capturing the stator's dynamic response. This approach not only provides a comprehensive understanding of both the free and forced vibrational behaviour of electric motor stators but also establishes a dependable framework offering valuable insights for mitigating vibrations and improving the overall electric motor performance.

Keywords: *experimental modal analysis, e-motor stator assembly, analytical structural dynamics, forced response.*

1. INTRODUCTION

Electric motor noise, vibration, and harshness (NVH) are critical concerns in modern powertrain development, with stator vibrations being a dominant source of acoustic emissions [1]. Predicting accurately the natural frequencies and mode shapes of a stator assembly is essential for understanding its dynamic response under electromagnetic excitation and avoiding resonances that can lead to excessive noise and structural fatigue. While numerical methods provide detailed modal and dynamic predictions, their computational expense remains a major limitation, especially for high-frequency analyses requiring fine meshes and small time steps [2], [3]. Prior reduced-order and analytical approaches [4]-[6] have been proposed, however, they typically rely on simplifying assumptions, such as reducing the problem to two dimensions or neglecting critical structural and geometric complexities of the stator assembly, thereby limiting their applicability.

This paper proposes an analytical modelling framework for the modal and dynamic analysis of electric motor stator assemblies based on the First-order Shear Deformation Stress Theory (FSDST). The proposed methodology offers a highly accurate, computationally efficient alternative to numerical approaches. By axially segmenting the assembly and introducing continuous functions to characterise the material properties across its thickness, the model effectively captures the effects of anisotropic parameters as well as dimensional variations. The displacement field is formulated using orthogonal Jacobi polynomial functions and the natural frequencies and mode shapes are computed via the Lagrangian energy method. The Newmark-β integration technique is then employed for the evaluation of the forced response of the system under an impulse excitation. The methodology is outlined in Section 2, and results of the analytical model are presented and assessed against experimental data in Section 3.

[*] ***Corresponding author***: *s.theodossiades@lboro.ac.uk*

2. METHODOLOGY

2.1 Mechanical Model and Material Characterisation

The stator assembly is modelled as a thick cylindrical shell of length L and radius R, divided into P segments, each with a thickness h_P and length L_P. This segmentation allows for the incorporation of dimensional variations within the cylindrical shell. To accurately represent the complex material properties of the assembly – including the stator windings, teeth, stator yoke, and cooling jacket or housing – carefully formulated continuous functions are introduced. These functions characterise the orthotropic nature of the stator lamination and the variation of material properties across the shell's thickness. More specifically, they comprehensively characterise the modulus of elasticity, shear modulus, Poisson's ratio, and density.

2.2 Displacement and Energy Equations

Through the assumptions that the shell displacements are small relatively to their thickness and that normal shear stresses are negligible, the displacement field can be expressed in accordance with first-order shear deformation shell theory (FSDST) as [7]:

$$\boldsymbol{u^p(x,\varphi,z,t) = u_0^p(x,\varphi,t) + z\beta_x^p(x,\varphi,t)} \quad (1)$$

$$\boldsymbol{v^p(x,\varphi,z,t) = v_0^p(x,\varphi,t) + z\beta_\varphi^p(x,\varphi,t)} \quad (2)$$

$$\boldsymbol{w^p(x,\varphi,z,t) = w_0^p(x,\varphi,t)} \quad (3)$$

where u, v, and w are the mid-surface displacements in the axial, circumferential and normal directions, and β_x and β_φ are the mid-surface rotations in the axial and circumferential directions, respectively. Once these functions are established, the FSDST is employed to express the kinetic energy T^P, potential energy U^P , and external work W^P associated with each segment, as follows:

$$U^p = \frac{R}{2}\int_0^{L_p}\int_{-h_p/2}^{h_p/2}\int_0^{2\pi}\left(\sigma_{xx}^p\varepsilon_x^p + \sigma_{\varphi\varphi}^p\varepsilon_\varphi^p + \tau_{x\varphi}^p\gamma_{x\varphi}^p + \tau_{xz}^p\gamma_{xz}^p + \tau_{\varphi z}^p\gamma_{\varphi z}^p\right)\left(1+\frac{z}{R}\right)d\varphi\,dz\,dx \quad (4)$$

$$T^p = \frac{R}{2}\int_0^{L_p}\int_{-h_p/2}^{h_p/2}\int_0^{2\pi}\rho_p\left(\dot{u}_p^2 + \dot{v}_p^2 + \dot{w}_p^2\right)\left(1+\frac{z}{R}\right)d\varphi\,dz\,dx \quad (5)$$

$$W^p = \frac{R}{2}\int_0^{L_p}\int_{-h_p/2}^{h_p/2}\int_0^{2\pi}\left(f_u^p u_0^p + f_v^p v_0^p + f_w^p w_0^p + f_{\beta_x}^p\beta_x^p + f_{\beta_\varphi}^p\beta_\varphi^p\right)\left(1+\frac{z}{R}\right)d\varphi\,dz\,dx \quad (6)$$

where σ, ε, τ and γ represent the normal stress, normal strain, shear stress and shear strain in each direction for the p-th segment, ρ is the density and f denotes the external force.

2.3 Boundary and Continuity Enforcement

To satisfy continuity between adjacent segments and ensure that transverse and shear displacements at the end of one segment match the start of the next segment, artificial massless springs are introduced. Similarly, artificial springs are incorporated at each end of the cylindrical shell, allowing for any possible boundary condition to be imposed, by varying the appropriate spring stiffnesses. The energy stored in the artificial continuity and boundary springs is calculated according to the penalty method [8], denoted as U_c and U_b, respectively.

2.4 Eigenvalue Analysis

Having established the energy formulations, the Lagrangian energy function $\mathcal{L}$, may be expressed as:

$$\mathcal{L} = \sum_{p=1}^{P}(T^p - U^p + W^p) - \sum_{p=1}^{P-1}U_c^{p,p+1} - U_b \quad (7)$$

Minimising the Lagrangian energy function with respect to each of the generalised coordinate variable yields:

$$\boldsymbol{M\ddot{q} + Kq = F} \quad (8)$$

where $\boldsymbol{q}$ is the global generalised coordinate vector, $\boldsymbol{M}$ and $\boldsymbol{K}$ are respectively the mass and stiffness matrices and $\boldsymbol{F}$ is the external load vector. For the eigenvalue analysis, external work is neglected, and the system is assumed to undergo free harmonic motion, i.e. $\boldsymbol{F = 0}$ and $\boldsymbol{q(t) = \bar{q}e^{i\omega t}}$. Substituting these into Equation 8 yields:

$$\boldsymbol{[-\omega_{nat}^2 M + K]\bar{q} = 0} \quad (9)$$

The solution of the above expression returns the natural frequencies of the system, ω_{nat} and their corresponding eigenvectors, $\bar{\boldsymbol{q}}$.

2.5 Forced Response

For the evaluation of the dynamic response of the system under impulse load, the Newmark-β integration method was utilised, due to its numerical stability, computational efficiency and versatility [9]. Having obtained the modal damping ratios from the Experimental Modal Analysis (EMA) performed on the actual system, the damping matrix was constructed following the Rayleigh damping method. The applied force in the analytical model, at location (x_0, θ_0, z_0), is expressed as:

$$f_w(x,\theta,t) = A(t)\delta(x-x_0)\delta(\theta-\theta_0)\delta(z-z_0) \quad (10)$$

where $A(t)$ denotes the time-dependent force amplitude obtained experimentally, and δ is the Dirac delta function, which allows for spatial localisation of the applied force.

3. RESULTS AND DISCUSSION

Having applied the methodology outlined above to a real stator assembly from an electric vehicle powertrain, this section presents and discusses some of the results obtained, with comparisons against experimental data. **Table 1** presents the results of the EMA compared against the analytical natural frequency predictions for the first five vibration modes of the system. The average error across the presented modes is -1.03% (maximum error 7.54%), thus within an acceptable range, confirming that the analytical method effectively captures the modal characteristics of the complex stator assembly, and that the assumptions utilised within the model are successful. The accuracy of the model is also shown in **Figure 1**, with the analytically derived cylindrical mode shapes being in very close conformity with the ones obtained from the EMA.

Table 1. Comparison of EMA results with analytical natural frequency predictions

Mode *(n,m)*	Exp. (Hz)	Damp. (%)	Ana. (Hz)	Error (%)
(2,0)	604	1.11	609	0.85
(3,0)	1692	0.99	1589	-6.07
(2,1)	2088	1.03	2172	4.00
(3,1)	2598	1.05	2692	3.61
(4,0)	2976	1.56	2751	-7.54

Finally, the experimental and analytical acceleration signals following the impulse excitation described in Section 2 are presented in the time-domain in **Figure 2**. It can be observed that both systems exhibit a sharp initial acceleration peak due to the applied impulse, followed by rapidly decaying oscillatory motion, as the stator assembly is allowed to come to rest. The peak acceleration values in both signals are similar, indicating that the application of the excitation in the analytical model is consistent with the experiment. There is however a slight discrepancy in the amplitude decay rate, which could be justified by the simplified damping representation implemented in the analytical model, as well as additional energy dissipation in the real system. This energy dissipation could be a result of friction at the interfaces between the assembly's layers or between the system and the elastic supports used to approximate free boundary conditions.

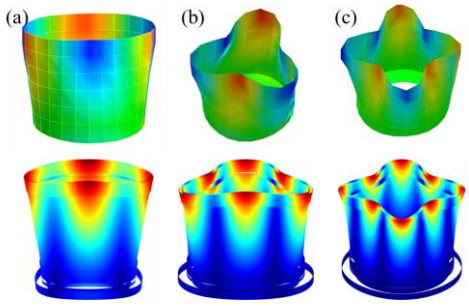

Figure 1. Comparison of experimentally obtained mode shapes (top) with analytically derived ones (bottom) for mode (a) (2,0), (b) (3,0) and (c) (4,0).

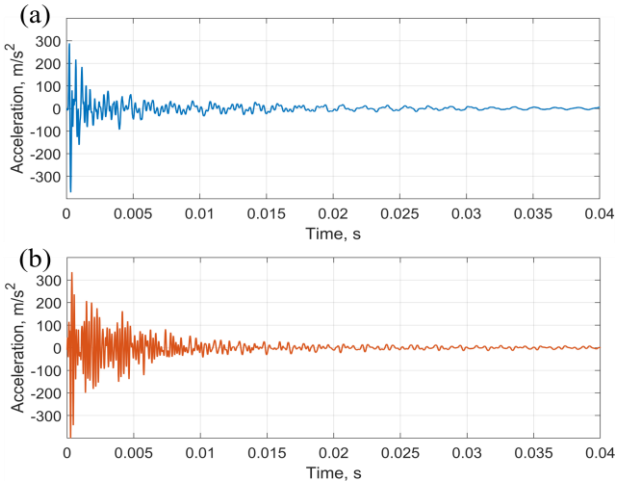

Figure 2. Experimentally obtained (a) and analytically predicted (b) acceleration response at a random location mode on the stator assembly following impulse excitation.

The Frequency Response Function (FRF) of the acceleration signals, shown in **Figure 3**, provides further insight into the accuracy of the analytical model in capturing the dynamic behaviour of the stator assembly. The dominant resonant peaks predicted analytically align well with those observed experimentally, confirming that the developed methodology accurately identifies the primary vibration modes of the structure. The discrepancies in the locations of the peaks are mostly explained by the errors in the calculation of the natural frequencies. Additionally, in the experimental signal there appear to be contributions in the range of 800-1350 Hz, as well as 1750-2000 Hz, which are caused by the degenerate mode pairs of vibration modes (2,0) and (3,0), but due to geometric asymmetries in the real system they have different frequencies. These asymmetries cannot be captured by the cylindrical analytical model hence there is no contribution

at those frequencies. Furthermore, minor discrepancies at higher frequencies may again be attributed to the assumptions introduced by the Rayleigh damping method and may be minimised through further damping refinement.

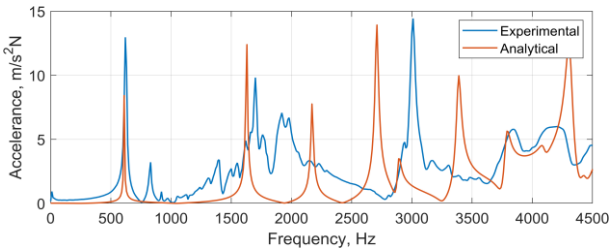

Figure 3. Acceleration Frequency Response Function (FRF) of the structure following impulse excitation.

4. CONCLUSIONS

This work introduces an accurate, yet highly computationally efficient framework for identification of the modal characteristics and the dynamic response analysis of electric motor stator assemblies. The overall agreement between analytical and experimental results demonstrates the effectiveness of the proposed methodology in predicting the dynamic behaviour of complex stator assemblies. The natural frequency and mode shape predictions of the analytical model are in excellent agreement with EMA results, with a maximum error of 7.54%. The dynamic response of the system to an impulse excitation is captured with great qualitative agreement, considering the differences in peak amplitudes can be attributed to damping simplifications, while the frequency deviations are a direct result of the deviations in natural frequency predictions. However, further refinement of damping parameter estimation could enhance the model's predictive capability. Incorporating additional experimental data to fine-tune damping coefficients or employing a more detailed dissipation model could further improve the accuracy of time-domain responses.

Despite these minor discrepancies, the developed analytical approach provides a computationally efficient and reliable tool for modal analysis of stator assemblies. Its ability to closely match experimental results highlights its potential for early-stage NVH assessment and optimization in electric powertrains.

5. ACKNOWLEDGMENTS

The authors would like to thank Arrival Ltd for their technical support, as well as the EPSRC [EP/T518098/1 – DTP 2020-2021 & EP/V053353/1 – Automotive electric powertrain whistling and whining: fundamental root cause analysis to novel solutions], the UKRI [2585407 – Electric motor and transmission coupled vibro-acoustics of electric powertrains] and the Loughborough University Doctoral College for supporting this work.

6. REFERENCES

[1] N. Morris *et al*, "4 - tribodynamic analysis of electric vehicle powertrains," in *Electric Vehicle Tribology*, L. I. Farfan-Cabrera and A. Erdemir, Eds. 2024. DOI: 10.1016/B978-0-443-14074-7.00004-2.

[2] X. Liang *et al*, "Comparative Study of Classical and Mutually Coupled Switched Reluctance Motors Using Multiphysics Finite-Element Modeling," *IEEE Transactions on Industrial Electronics,* vol. 61, *(9),* pp. 5066–5074, 2014. DOI: 10.1109/TIE.2013.2282907.

[3] Y. S. Wang *et al*, "Electromagnetic noise analysis and optimization for permanent magnet synchronous motor used on electric vehicles," *EC,* vol. 38, *(2),* pp. 699, 2020. DOI: 10.1108/ec-02-2020-0070.

[4] P. Andreou *et al*, "Analytical Multiphysics Methodology to Predict Vibroacoustics in PMSMs Combining Tangential Electromagnetic Excitation and Tooth Modulation Effects," *IEEE Transactions on Transportation Electrification,* vol. 10, *(3),* pp. 5997–6009, 2024. DOI: 10.1109/TTE.2023.3325350.

[5] R. Sun *et al*, "A novel forward computational modal analysis method of the motor stator assembly considering core lamination and winding stacking," *Mechanical Systems and Signal Processing,* vol. 208, pp. 110920, 2024. DOI: 10.1016/j.ymssp.2023.110920.

[6] P. Andreou *et al*, "Reduced Order Model for Modal Analysis of Electric Motors Considering Material and Dimensional Variations," SAE Technical Paper 2024-01-2945, 2024, https://doi.org/10.4271/2024-01-2945.

[7] M. S. Qatu, "Accurate equations for laminated composite deep thick shells," *Int. J. Solids Structures,* vol. 36, *(19),* pp. 2917–2941, 1999. DOI: 10.1016/S0020-7683(98)00134-6.

[8] L. Lu *et al*, "Dynamic analysis of stepped functionally graded conical shells with general boundary restraints using Jacobi polynomials-Ritz method," *Thin-Walled Structures,* vol. 204, pp. 112304, 2024. DOI: 10.1016/j.tws.2024.112304.

[9] C. Gao *et al*, "Free and forced vibration analysis of uniform and stepped combined conical-cylindrical-spherical shells: A unified formulation," *Ocean Eng.,* vol. 260, pp. 111842, 2022. DOI: 10.1016/j.oceaneng.2022.111842.